

**Systemic LPS-induced neuroinflammation increases the susceptibility for proteasome inhibition-induced degeneration of the nigrostriatal pathway**

Deneyer, Lauren; Albertini, Giulia; Bentea, Eduard; Massie, Ann

*Published in:*  
Parkinsonism and Related Disorders

*DOI:*  
[10.1016/j.parkreldis.2019.09.025](https://doi.org/10.1016/j.parkreldis.2019.09.025)

*Publication date:*  
2019

*License:*  
CC BY-NC-ND

*Document Version:*  
Accepted author manuscript

[Link to publication](#)

*Citation for published version (APA):*  
Deneyer, L., Albertini, G., Bentea, E., & Massie, A. (2019). Systemic LPS-induced neuroinflammation increases the susceptibility for proteasome inhibition-induced degeneration of the nigrostriatal pathway. *Parkinsonism and Related Disorders*, 68, 26-32. <https://doi.org/10.1016/j.parkreldis.2019.09.025>

**Copyright**

No part of this publication may be reproduced or transmitted in any form, without the prior written permission of the author(s) or other rights holders to whom publication rights have been transferred, unless permitted by a license attached to the publication (a Creative Commons license or other), or unless exceptions to copyright law apply.

**Take down policy**

If you believe that this document infringes your copyright or other rights, please contact [openaccess@vub.be](mailto:openaccess@vub.be), with details of the nature of the infringement. We will investigate the claim and if justified, we will take the appropriate steps.

1 **Systemic LPS-induced neuroinflammation increases the susceptibility for**  
2 **proteasome inhibition-induced degeneration of the nigrostriatal pathway**

3 Lauren Deneuer<sup>1</sup>, Giulia Albertini<sup>2</sup>, Eduard Bentea<sup>1</sup>, and Ann Massie<sup>1</sup>

4 <sup>1</sup>Department of Pharmaceutical Biotechnology and Molecular Biology, Center for Neurosciences, Vrije  
5 Universiteit Brussel, Brussels, Belgium

6 <sup>2</sup>Department of Pharmaceutical Chemistry and Drug Analysis, Center for Neurosciences, Vrije  
7 Universiteit Brussel, Brussels, Belgium

8

9 Correspondence should be addressed to:

10 Prof. Dr. Ann Massie

11 Vrije Universiteit Brussel

12 Department of Pharmaceutical Biotechnology and Molecular Biology

13 Center for Neurosciences

14 Laarbeeklaan 103

15 Brussels, Belgium

16 Ann.Massie@vub.be

17 +32 2 477 45 02 (TEL)

18

19

20

21

22

23

24

25 **KEYWORDS:** Parkinson's disease, lipopolysaccharide, lactacystin, dopamine

26 **ABSTRACT:**

27 **Introduction:** Besides proteasome dysfunction, neuroinflammation is a common feature in the  
28 pathogenesis of Parkinson's disease (PD). Accordingly, peripheral inflammation has been  
29 shown to increase the susceptibility of the brain for nigrostriatal degeneration by inducing  
30 activation of glial cells and release of pro-inflammatory cytokines in the brain. Given that  
31 current animal models of PD fail to recapitulate the pathophysiology occurring in idiopathic  
32 PD, the aim of this study was to combine two pathogenic mechanisms (i.e. neuroinflammation  
33 and proteasome inhibition) to create a dual-hit mouse model of PD.

34 **Methods:** We repeatedly injected mice with a low dose of LPS (250 µg/kg/day i.p. for four  
35 days) to induce neuroinflammation, followed by a unilateral intranigral injection of lactacystin  
36 (LAC; 3 µg). Seven days later, mice were evaluated behaviorally to assess locomotion, anxiety-  
37 and depressive-like behavior. Nigrostriatal degeneration was analyzed by measuring striatal  
38 dopamine loss as well as loss of nigral dopaminergic neurons. Neuroinflammation was  
39 confirmed by quantifying microglial cells in the substantia nigra (SN) and cytokine expression  
40 in the striatum.

41 **Results:** Repeated systemic LPS injections increase the number of microglial cells in the SN  
42 and induce a mixed profile of pro- and anti-inflammatory cytokines in the striatum without  
43 affecting the integrity of the nigrostriatal pathway. Systemic LPS-induced neuroinflammation,  
44 however, increases the susceptibility of the nigrostriatal pathway for LAC-induced  
45 degeneration.

46 **Conclusion:** Recapitulating two relevant etiopathogenic mechanisms of PD -  
47 neuroinflammation and proteasome inhibition-, we propose this dual-hit model as a relevant  
48 mouse model for PD that could be used to investigate potential therapeutic targets.

49

50

## 51 INTRODUCTION

52 Parkinson's disease (PD) is an age-related debilitating neurodegenerative disorder  
53 characterized by a selective and gradual loss of dopaminergic innervations from the Substantia  
54 Nigra (SN) pars compacta (SNpc) to the striatum. Over the years, findings from  
55 epidemiological studies, *post-mortem* PD brains and animal PD models have provided evidence  
56 to support the role for central and peripheral inflammation in the pathogenesis of PD [1].  
57 Microglia participate to central nervous system homeostasis by removing debris and responding  
58 to injury, while synthesizing a variety of cytokines and neurotrophic factors. However, in the  
59 context of neurodegenerative disorders, it is hypothesized that high levels of pro-inflammatory  
60 mediators released by chronically activated microglia, damage neurons and further activate  
61 microglia, resulting in a feed-forward inflammatory cycle [2]. Preclinical studies demonstrated  
62 that neuroinflammation induced by single or repeated systemic lipopolysaccharide (LPS)  
63 exposure replicates some characteristics of PD: a prolonged and widespread microglial  
64 activation results in progressive loss of dopaminergic neurons in the nigrostriatal system in  
65 days, weeks or months depending on the paradigm used [3]. Moreover, microglia react upon  
66 LPS exposure and the subsequent increased cytokine levels by adopting an atypical or primed  
67 state; a phenomenon also observed in the aged central nervous system. These primed microglia  
68 could exert an exaggerated pro-inflammatory response, thereby enhancing the  
69 neurodegenerative effects of later exposure to a second stimulus [4].

70 Multiple-hit animal PD models might represent a valid alternative to well-established models  
71 of PD. For instance, novel models of idiopathic PD are generated by exposure to a combination  
72 of the classical toxins/agents such as LPS, MPTP, 6-OHDA, rotenone, etc [5]. In the early  
73 2000s, an intriguing new factor has been associated with the pathogenesis of PD. *Post-mortem*  
74 data from sporadic PD patients indicated that proteasome function is impaired in the SN,  
75 including loss of 20S core alpha subunits, decreased expression of 19S and general loss of all

76 three peptidase activities. The underlying cause of proteasome dysfunction in PD has not been  
77 elucidated [6,7]. A recent approach to model proteasome dysfunction *in vivo* has been the use  
78 of the toxin lactacystin (LAC), a selective proteasome inhibitor that inhibits all three peptidase  
79 activities of the 20S proteasome. LAC has been successfully used in rats and mice as its nigral  
80 administration produces a fast-onset PD-like phenotype, including  $\alpha$ -synuclein accumulation,  
81 dopaminergic cell loss and behavioral deficits [6,8,9]. Despite neuroinflammation and  
82 proteasome dysfunction being two significant hallmarks of many neurodegenerative diseases,  
83 the relationship between both factors is poorly understood. In this study, we evaluated the effect  
84 of prior exposure to an inflammogen (i.e. LPS) on proteasome inhibition-induced parkinsonism  
85 in mice.

## 86 MATERIAL AND METHODS

### 87 Animals

88 Male C57BL/6J mice (11-12 weeks of age; Charles River Laboratories) were group-housed (2-  
89 6 mice/cage) in a 14/10 h light/dark cycle with free access to food and tap water. Temperature  
90 (21-25 °C) and relative humidity (30-60 %) were maintained constant during the experiments,  
91 which were carried out according to the Belgian animal welfare legislation (Royal Decree of  
92 29 May 2013) and the regulations covering animal experimentation in the EU (European  
93 Communities Council Directive 2010/63/EU). The Ethical Committee for Animal Experiments  
94 (Vrije Universiteit Brussel) approved the experiments.

### 95 Induction of peripheral inflammation

96 Peripheral inflammation was induced by repeated intraperitoneal (i.p.) LPS (*Escherichia coli*,  
97 O55:B5, Sigma-Aldrich) injections of 250  $\mu$ g/kg over four consecutive days while control mice  
98 received i.p. injections of vehicle (physiological saline, 0.9% w/v of NaCl). Solutions were  
99 made freshly before administration. Prior to each injection, mice were weighed, and body  
100 temperature was measured to evaluate LPS-induced sickness behavior.

## 101 **Stereotaxic surgery**

102 Mice were anesthetized (i.p. injection of a mixture of ketamine (100 mg/kg; Ketamine 1000  
103 Ceva, Ceva Sante Animale) and xylazine (10 mg/kg; Rompun 2%, Bayer N.V)) and positioned  
104 in an Ultra Precise Small Animal Stereotaxic Frame (David Kopf Instruments). A small hole  
105 was made through the skull above the left SNpc (AP -3.0, LM -1.0, DV -4.5 from Bregma). A  
106 volume of 1.5  $\mu$ l freshly-dissolved LAC (2  $\mu$ g/ $\mu$ l in NaCl 0.9%; Cayman Chemical) was  
107 injected at a flow rate of 0.5  $\mu$ l/min into the left SNpc. Sham-operated mice received the same  
108 volume of saline. After injection, the syringe was left in place for five additional min, and then  
109 slowly removed. The skin was sutured, and mice received 4 mg/kg ketoprofen subcutaneously  
110 (Ketofen, Merial) for post-operative analgesia.

## 111 **Behavioral assessment**

112 Seven days after LAC lesion, mice underwent behavioral assessment to test motor dysfunction  
113 using the rotarod and open field test, and anxiety- and depressive-like behavior using the open  
114 field, light-dark and tail suspension test [6,10] as described in Supplementary material.

## 115 **Neurochemical analysis of striatal dopamine content**

116 Striatal content of dopamine and the selected metabolites 3,4-dihydroxyphenylacetic acid  
117 (DOPAC) and homovanillic acid (HVA) were measured using HPLC (see Supplementary  
118 material for more details).

## 119 **Immunohistochemistry**

120 The caudal part of the brain was post-fixed for three days in 4% paraformaldehyde and sliced  
121 into 40  $\mu$ m vibratome sections to immunohistochemically detect tyrosine hydroxylase (TH) and  
122 ionized calcium binding adapter molecule 1 (Iba1), using rabbit anti-TH (1/2000; AB152;  
123 Millipore) and rabbit anti-Iba1 antibody (1/1000; 019-19741, RRID: AB\_839504), and  
124 employing the Vectastain ABC kit (Vector Laboratories). The mean number of TH+ profiles  
125 per mice was counted blindly in six serial sections throughout the rostro-caudal extent of the

126 SNpc (-2.92 mm to -3.60 mm relative to Bregma [11]). Similarly, the number of Iba1+  
127 profiles/mm<sup>2</sup> was evaluated in three serial sections covering the SN. Immunoreactivity was  
128 visualized using 3,3'-diaminobenzidine as chromogen. Microscopic analysis and cell count of  
129 the sections were performed using ImageJ software (U.S. National Institutes of Health,  
130 Bethesda).

### 131 **Western Blot analysis**

132 In a separate cohort of mice, striatal TH expression was quantified using semi-quantitative  
133 Western blotting, using primary rabbit anti-TH antibody (1/2000, AB152) and enhanced  
134 chemiluminescence (ECL prime, GE Healthcare) as described in Supplementary material.  
135 Optical densities of TH-immunoreactive bands were normalized to those of the total amount of  
136 proteins loaded, visualized on the same membrane (SERVA Purple, Serva Electrophoresis  
137 GmbH).

### 138 **Real-time PCR**

139 IL-1 $\beta$ , TNF- $\alpha$ , nitric oxide synthase (NOS2) and arginase 1 (Arg1) mRNA expression was  
140 quantified using real-time polymerase chain reaction (qPCR). Total RNA was extracted from  
141 the striatum (RNeasy<sup>®</sup> Lipid Tissue Mini Kit; Qiagen) and the RNA concentration and purity  
142 were determined using the Nanodrop ND-1000 UV-Vis Spectrophotometer (Thermo Fisher).  
143 After cDNA synthesis (iScript<sup>™</sup> cDNA Synthesis Kit, Bio-Rad Laboratories), real-time PCR  
144 was performed using the StepOnePlus<sup>™</sup> qPCR system (Applied Biosystems; Foster City) in  
145 combination with TaqMan<sup>®</sup> reagents (Applied Biosystems) and TaqMan<sup>®</sup> Gene Expression  
146 Assays (more details in Supplementary material). The results were processed according to the  
147 2- $\Delta\Delta$ CT method and mRNA expression levels were expressed as fold changes relative to  
148 vehicle-treated mice and normalized against the geometric means of Bcl2113 mRNA  
149 expression levels.

### 150 **Statistical analysis**

151 Data were expressed as mean  $\pm$  Standard Error of the Mean (SEM). Statistical analysis was  
152 performed using GraphPad Prism 6.01 software. To study one variable within one group of  
153 animals, we employed Mann Whitney U test. Two paired groups were analyzed using the two-  
154 sided Wilcoxon matched-pairs signed-rank test. For analysis of multiple variables within  
155 multiple groups of animals, we applied two-way ANOVA followed by Tukey's *post hoc* test  
156 on the significant main effects. The  $\alpha$ -value was set at 0.05.

## 157 **RESULTS**

### 158 **Four daily LPS injections induce changes in body weight**

159 Mice were injected for four consecutive days with either vehicle or LPS and were sacrificed on  
160 the fifth day (96 hours after the first injection). Body weight and temperature were measured  
161 24 hours after each injection to assess sickness behavior. At the end of the four-day treatment  
162 period, LPS-treated mice had a significant decrease in body weight compared to baselines (i.e.  
163 before the first injection) [ $p < 0.0001$ ], contrary to vehicle-injected mice [ $p > 0.05$ , Figure 1A].  
164 However, whereas the first [ $p < 0.0001$ ] and second [ $p < 0.01$ ] LPS injection resulted in a  
165 significant decrease in body weight after 24 hours, the third and fourth LPS injection induced  
166 a significant increase in body weight compared to vehicle injection [ $p < 0.05$ , Figure 1B].  
167 Repeated LPS treatment did not induce changes in body temperature as no significant  
168 differences could be observed at the end or during the four-day treatment between LPS- and  
169 vehicle-treated mice [ $p > 0.05$ , Figure 1C, D].

### 170 **Repeated LPS injections activate microglial cells, without affecting the integrity of the** 171 **nigrostriatal pathway**

172 We observed a significant increase in the number of Iba1<sup>+</sup> cells per mm<sup>2</sup> in the SN after the  
173 four-day LPS treatment, compared to vehicle treatment [VEH:  $339.9 \pm 8.774$  cells/mm<sup>2</sup>, LPS:  
174  $402.3 \pm 22.80$  cells/mm<sup>2</sup>,  $U = 5.000$ ,  $p = 0.0221$ ; Figure 2A, B]. The mRNA expression levels  
175 of IL-1 $\beta$  [6.6-fold,  $p = 0.0006$ ] and Arg1 [3.5-fold,  $p = 0.0401$ ] were significantly higher in the



176 striatum of the LPS group compared to the control group, whereas no significant differences  
177 were observed for TNF- $\alpha$  and NOS2 [ $p > 0.05$ , Figure 2C]. Four repeated LPS injections do  
178 neither affect the striatal TH protein expression [ $p > 0.05$ ; Figure 2D] nor the number of TH+  
179 profiles in the SNpc [ $p > 0.05$ ; Figure 2E], as compared to vehicle-treated mice.

### 180 **LPS-induced neuroinflammation potentiates nigrostriatal degeneration induced by** 181 **proteasome inhibition**

182 The total number of Iba1+ cells was evaluated in the SN to study the consequences of LPS pre-  
183 treatment on LAC-induced neuroinflammation. A significant increase in the number of Iba1+  
184 cells could be detected in the ipsilateral SN after intranigral LAC injection, compared to sham-  
185 treatment [lesion factor:  $F(1,18) = 4.993$ ,  $p = 0.0384$ ], independent of LPS pre-treatment (Figure  
186 3A). We next investigated whether prior systemic LPS-induced neuroinflammation increases  
187 susceptibility of dopaminergic neurons to proteasome inhibition-induced degeneration.  
188 Immunohistochemical analyses revealed that intranigral LAC administration led to a significant  
189 loss of TH-expressing cells in the ipsilateral SNpc [lesion factor:  $F(1,37) = 8.273$ ,  $p = 0.0066$ ;  
190 Figure 3B, C]. In addition, neurodegeneration induced by LAC was more pronounced in mice  
191 pre-treated with LPS compared to vehicle, as *post hoc* analysis revealed a significant decrease  
192 in TH+ cells only in the LPS group. Interestingly, LPS pre-treatment significantly enhanced the  
193 LAC-induced loss of dopamine in the ipsilateral striatum [lesion factor:  $F(1, 37) = 35.05$ ,  $p <$   
194  $0.0001$ ; treatment factor:  $F(1, 37) = 4.527$ ,  $p = 0.041$ ; Figure 3D]. Whereas LAC lesion induced  
195 a significant loss of striatal dopamine content in both vehicle- and LPS-treated mice, LPS pre-  
196 treatment resulted in a significantly lower dopamine content after LAC lesion, compared to  
197 vehicle pre-treatment. As an alternative measure for neuronal function, we assessed dopamine  
198 turnover (DOPAC+HVA/dopamine) in the ipsilateral striatum. There was a significant  
199 interaction between lesion and treatment [interaction factor:  $F(1,37) = 4.274$ ,  $p = 0.0458$ ; Figure

200 3E], with the dopamine turnover being significantly increased in the LPS LAC group compared  
201 to all other experimental groups.

202 **Systemic LPS injection has only minor effects on proteasome inhibition-induced changes**  
203 **in motor function, without affecting depressive-like behavior**

204 LAC-injected mice displayed a global impairment in motor coordination and balance compared  
205 to sham-treated mice on the rotarod test [lesion factor:  $F(1,49) = 19.86$ ,  $p < 0.0001$ ; Figure 4A],  
206 which was less pronounced after LPS treatment. In contrast, a significant increase in distance  
207 traveled, was seen in the open field test after LAC treatment [lesion factor:  $F(1,49) = 15.11$ ,  $p$   
208  $= 0.0003$ ; Figure 4B], which was more evident in the LPS pre-treated group. For all behavioral  
209 tests described, we failed to reveal any effect related to anxiety-like behavior as seen in the  
210 latency to exit and time spent outside of the shelter in the light dark test (Figure 4C, D) as well  
211 as time spent in the center of the open field test (Figure 4E). Finally, we investigated depressive-  
212 like symptoms using the tail suspension test. Interestingly, we could observe a paradoxical  
213 decrease in immobility time after LAC [lesion factor:  $F(1,35) = 10.52$ ,  $p = 0.0026$ ; Figure 4F],  
214 unrelated to LPS or vehicle pre-treatment.

215 **DISCUSSION**

216 Exposure to LPS - an inflammogen known to activate microglia and to induce widespread  
217 (neuro)inflammation depending on the dose and paradigm used - can selectively induce  
218 dopaminergic neuron loss in animals [1]. Microglia produce pro-inflammatory mediators and  
219 reactive species, which, when present in excess or over a prolonged period of time, could lead  
220 to neuronal damage and in turn contribute to sustained inflammation in PD. Microglia are  
221 considered pro-inflammatory if they produce higher levels of pro-inflammatory factors such as  
222 IL-1 $\beta$ , TNF- $\alpha$  or iNOS, while increased levels of Arg1, Ym1 and IL-10 indicate a more anti-  
223 inflammatory phenotype. Badshah *et al.* (2016) described increased Iba1 expression in the  
224 hippocampus and cortex after seven days of 250  $\mu\text{g}/\text{kg}$  LPS treatment together with increased

225 protein expression of IL-1 $\beta$ , TNF- $\alpha$  and NOS2 [12]. Our data show that daily administration of  
226 LPS 250  $\mu$ g/kg for four days resulted in a significantly increased number of Iba1+ cells in the  
227 SN. In addition, increased striatal mRNA levels of the pro-inflammatory IL-1 $\beta$  and anti-  
228 inflammatory Arg1 were detected 24 hours after the last LPS challenge. This mixed  
229 inflammatory profile was reported before by Beier et al. (2017), who showed increases in the  
230 pro-inflammatory markers (iNOS, IL-1 $\beta$ , TNF- $\alpha$ , IL-6) on day five after four daily LPS  
231 injections of 1 mg/kg followed by a mixed expression profile of pro- and anti-inflammatory  
232 cytokines on day 19, ending with a predominantly anti-inflammatory profile on day 36 together  
233 with a total cessation of neuronal loss [13].

234 The mixed inflammatory profile that we observe in the striatum after four consecutive LPS  
235 injections possibly reflects a mixed systemic inflammatory profile and could as such explain  
236 the transient weight loss in these mice: only the first and second LPS challenge induced a robust  
237 change in body weight, while the third and fourth challenge did not lead to further decreases  
238 and mice even seemed to start recovering, according to the observation made by Püntener et al.  
239 (2012) [14]. Besides sickness behavior, systemic LPS injections were shown to trigger  
240 progressive neurodegeneration in the SN especially at higher doses. Whereas a single systemic  
241 LPS (5mg/kg, i.p.) injection was reported to induce a strong inflammatory response and a slow  
242 progressive loss of TH+ neurons in the SN after 10 months of treatment [3], repeated 1 mg/kg  
243 LPS injections significantly reduced the amount of TH+ cells after 19 days [15], with no  
244 neuronal loss present on day 5 [13]. We therefore examined the possible deleterious effects of  
245 four systemic low-dose LPS injections on the nigrostriatal pathway and found no loss of  
246 dopaminergic neurons in the SNpc nor decreased striatal TH expression levels, indicating that  
247 this paradigm of LPS treatment does not affect the nigrostriatal pathway, despite the significant  
248 nigral microglial activation. The indication of a mixed pro- and anti-inflammatory profile in the

249 striatum could provide an explanation for this intact nigrostriatal pathway, as anti-inflammatory  
250 cytokines might gain the upper hand and protect against LPS-induced degeneration.

251 Prolonged systemic inflammation can give rise to hypo- (tolerance) as well as hyper- (priming)  
252 innate immune responses in the brain in response to a subsequent stimulus. Indeed, studies  
253 with double-hit animal models have shown that local or systemic application of bacterial LPS  
254 in both single or repeated challenges can aggravate toxin-induced neurodegeneration in models  
255 of PD [16–21]. In this study we administered the proteasome inhibitor LAC as a second  
256 stimulus after four consecutive injections of LPS. According to previous reports, we showed  
257 that local administration of LAC to the SN leads to degeneration of the nigrostriatal pathway  
258 [6,8,9]. Moreover, we report that seven days after intranigral LAC injection a significant  
259 increase in number of microglial cells is present in the SN compared to sham surgery,  
260 suggesting that proteasome inhibition and concomitant dopaminergic neurodegeneration  
261 triggers microglial activation. When mice were pre-treated with LPS prior to LAC exposure,  
262 we observed an enhancement of nigrostriatal degeneration, suggesting a sensitizing effect of  
263 LPS, in line with previous work in the MPTP [16], rotenone [22], paraquat [20] and 6-OHDA  
264 models [17,21]. In addition to striatal dopamine loss, a significant increase in dopamine  
265 turnover in the ipsilateral striatum was detected exclusively in the LPS pre-treated LAC-  
266 lesioned mice. Past research postulated that an increased dopamine turnover is one of the  
267 functional compensatory changes, conserving the normal motor function in PD, arising when  
268 dopamine depletion reached a certain threshold [23,24]. Local administration of LAC to the  
269 nigrostriatal pathway induces PD-related motor and non-motor symptoms [6]. Consistent with  
270 previous studies investigating the effect of nigrostriatal proteasome inhibition in rats [25–27]  
271 and mice [6,9], we observed strong impairment in rotarod performance in LAC-injected mice.  
272 This motor deficit was not affected by LPS pre-treatment, possibly as a result of the elevated  
273 dopamine turnover which could compensate for the dopamine depletion and related motor

274 impairment. In contrast, the open field test revealed an increase in spontaneous motor activity  
275 following LAC lesion, suggesting hyperkinetic behavior. Multiple studies discovered that  
276 unilateral intracerebral administration of a neurotoxin (i.e. MPTP, rotenone, epoxomicin and  
277 LAC) may induce hyperactivity of surviving dopaminergic neurons in the ipsilateral SNpc,  
278 which eventually results in selective increased firing frequency and consequent hyperkinetic  
279 behavior [6,28]. Besides motor symptoms, PD is also characterized by non-motor symptoms  
280 such as anxiety and depression, which are important determinants for the patient's quality of  
281 life. No differences could be noticed in the light-dark test and in the open field test between  
282 both treatment and lesion groups. These results should be interpreted with caution since both  
283 the open field and the light-dark test can be biased by the hyperactive behavior that was  
284 observed in LAC-treated animals. Consistent with the results of the open field test, we also  
285 noted an increased restlessness of both LPS- and vehicle-treated LAC-lesioned mice in the tail  
286 suspension test, suggesting hyperactivity or an increased perseverance to engage in escape-  
287 oriented behavior [6]. Our current findings strengthen the hypothesis that nigrostriatal  
288 neuroinflammation induced by peripheral inflammation increases the susceptibility of the  
289 nigrostriatal dopaminergic pathway for proteasome inhibition-induced degeneration, thereby  
290 identifying a novel and relevant mouse model for studying PD.

## 291 **ACKNOWLEDGEMENTS**

292 We kindly thank Olaya Lara, Anke Van Quickelberghe, Ria Berckmans and Dinja De Win for  
293 their assistance. This work was supported by grants of the Vrije Universiteit Brussel (SRP40),  
294 Research Foundation-Flanders (FWO), the Queen Elisabeth Medical Foundation (GSKE) and  
295 Scientific Fund Willy Gepts.

## 296 **REFERENCES**

297 [1] G. Gelders, V. Baekelandt, A. Van der Perren, Linking Neuroinflammation and  
298 Neurodegeneration in Parkinson's Disease, Journal of Immunology Research. 2018

- 299 (2018) 1–12. doi:10.1155/2018/4784268.
- 300 [2] M. Liu, G. Bing, Lipopolysaccharide animal models for Parkinson’s disease.,  
301 Parkinson’s Disease. 2011 (2011) 327089. doi:10.4061/2011/327089.
- 302 [3] L. Qin, X. Wu, M.L. Block, Y. Liu, G.R. Breese, J.S. Hong, D.J. Knapp, F.T. Crews,  
303 Systemic LPS causes chronic neuroinflammation and progressive neurodegeneration,  
304 GLIA. 55 (2007) 453–462. doi:10.1002/glia.20467.
- 305 [4] C. Cunningham, Microglia and neurodegeneration: The role of systemic inflammation,  
306 Glia. 61 (2013) 71–90. doi:10.1002/glia.22350.
- 307 [5] S. Duty, P. Jenner, Animal models of Parkinson’s disease: A source of novel treatments  
308 and clues to the cause of the disease, British Journal of Pharmacology. 164 (2011) 1357–  
309 1391. doi:10.1111/j.1476-5381.2011.01426.x.
- 310 [6] E. Bentea, A. Van der Perren, J. Van Liefferinge, A. El Arfani, G. Albertini, T.  
311 Demuyser, E. Merckx, Y. Michotte, I. Smolders, V. Baekelandt, A. Massie, Nigral  
312 proteasome inhibition in mice leads to motor and non-motor deficits and increased  
313 expression of Ser129 phosphorylated alpha-synuclein, Frontiers in Behavioral  
314 Neuroscience. 9 (2015). doi:10.3389/fnbeh.2015.00068.
- 315 [7] K.S.P. McNaught, R. Belizaire, O. Isacson, P. Jenner, C.W. Olanow, Altered  
316 proteasomal function in sporadic Parkinson’s disease, Experimental Neurology. 179  
317 (2003) 38–46. doi:10.1006/exnr.2002.8050.
- 318 [8] M.H. Savolainen, K. Albert, M. Airavaara, T.T. Myöhänen, Nigral injection of a  
319 proteasomal inhibitor, lactacystin, induces widespread glial cell activation and shows  
320 various phenotypes of Parkinson’s disease in young and adult mouse, Experimental  
321 Brain Research. 235 (2017) 2189–2202. doi:10.1007/s00221-017-4962-z.
- 322 [9] W. Xie, X. Li, C. Li, W. Zhu, J. Jankovic, W. Le, Proteasome inhibition modeling nigral  
323 neuron degeneration in Parkinson’s disease, Journal of Neurochemistry. 115 (2010) 188–

- 324 199. doi:10.1111/j.1471-4159.2010.06914.x.
- 325 [10] E. Bentea, T. Demuyser, J. Van Liefferinge, G. Albertini, L. Deneyer, J. Nys, E. Merckx,  
326 Y. Michotte, H. Sato, L. Arckens, A. Massie, I. Smolders, Absence of system xc- in mice  
327 decreases anxiety and depressive-like behavior without affecting sensorimotor function  
328 or spatial vision, *Progress in Neuro-Psychopharmacology and Biological Psychiatry*.  
329 (2015). doi:10.1016/j.pnpbp.2015.01.010.
- 330 [11] Y.H. Fu, Y. Yuan, G. Halliday, Z. Rusznák, C. Watson, G. Paxinos, A cytoarchitectonic  
331 and chemoarchitectonic analysis of the dopamine cell groups in the substantia nigra,  
332 ventral tegmental area, and retrorubral field in the mouse, *Brain Structure and Function*.  
333 217 (2012) 591–612. doi:10.1007/s00429-011-0349-2.
- 334 [12] H. Badshah, T. Ali, S. ur Rehman, F. ul Amin, F. Ullah, T.H. Kim, M.O. Kim, Protective  
335 Effect of Lupeol Against Lipopolysaccharide-Induced Neuroinflammation via the p38/c-  
336 Jun N-Terminal Kinase Pathway in the Adult Mouse Brain, *Journal of Neuroimmune  
337 Pharmacology*. 11 (2016) 48–60. doi:10.1007/s11481-015-9623-z.
- 338 [13] E.E. Beier, M. Neal, G. Alam, M. Edler, L.J. Wu, J.R. Richardson, Alternative microglial  
339 activation is associated with cessation of progressive dopamine neuron loss in mice  
340 systemically administered lipopolysaccharide, *Neurobiology of Disease*. 108 (2017)  
341 115–127. doi:10.1016/j.nbd.2017.08.009.
- 342 [14] U. Püntener, S.G. Booth, V.H. Perry, J.L. Teeling, Long-term impact of systemic  
343 bacterial infection on the cerebral vasculature and microglia, *Journal of  
344 Neuroinflammation*. (2012). doi:10.1186/1742-2094-9-146.
- 345 [15] L.G. Bodea, Y. Wang, B. Linnartz-Gerlach, J. Kopatz, L. Sinkkonen, R. Musgrove, T.  
346 Kaoma, A. Muller, L. Vallar, D.A. Di Monte, R. Balling, H. Neumann,  
347 Neurodegeneration by Activation of the Microglial Complement-Phagosome Pathway,  
348 *Journal of Neuroscience*. 34 (2014) 8546–8556. doi:10.1523/JNEUROSCI.5002-

- 349 13.2014.
- 350 [16] S.L. Byler, G.W. Boehm, J.D. Karp, R.A. Kohman, A.J. Tarr, T. Schallert, T.M. Barth,  
351 Systemic lipopolysaccharide plus MPTP as a model of dopamine loss and gait instability  
352 in C57Bl/6J mice, *Behavioural Brain Research*. 198 (2009) 434–439.  
353 doi:10.1016/j.bbr.2008.11.027.
- 354 [17] J.B. Koprach, C. Reske-Nielsen, P. Mithal, O. Isacson, Neuroinflammation mediated by  
355 IL-1 $\beta$  increases susceptibility of dopamine neurons to degeneration in an animal model  
356 of Parkinson's disease, *Journal of Neuroinflammation*. 5 (2008) 1–12. doi:10.1186/1742-  
357 2094-5-8.
- 358 [18] L. Hritcu, A. Ciobica, M. Stefan, M. Mihasan, L. Palamiuc, T. Nabeshima, Spatial  
359 memory deficits and oxidative stress damage following exposure to lipopolysaccharide  
360 in a rodent model of Parkinson's disease, *Neuroscience Research*. 71 (2011) 35–43.  
361 doi:10.1016/j.neures.2011.05.016.
- 362 [19] C. Pintado, M.P. Gavilán, E. Gavilán, L. García-Cuervo, A. Gutiérrez, J. Vitorica, A.  
363 Castaño, R.M. Ríos, D. Ruano, Lipopolysaccharide-induced neuroinflammation leads to  
364 the accumulation of ubiquitinated proteins and increases susceptibility to  
365 neurodegeneration induced by proteasome inhibition in rat hippocampus, *Journal of*  
366 *Neuroinflammation*. 9 (2012) 1. doi:10.1186/1742-2094-9-87.
- 367 [20] E.N. Mangano, S. Hayley, Inflammatory priming of the substantia nigra influences the  
368 impact of later paraquat exposure: Neuroimmune sensitization of neurodegeneration,  
369 *Neurobiology of Aging*. (2009). doi:10.1016/j.neurobiolaging.2007.11.020.
- 370 [21] M.C. Pott Godoy, R. Tarelli, C.C. Ferrari, M.I. Sarchi, F.J. Pitossi, Central and systemic  
371 IL-1 exacerbates neurodegeneration and motor symptoms in a model of Parkinson's  
372 disease, *Brain*. (2008). doi:10.1093/brain/awn101.
- 373 [22] H.M. Gao, J.S. Hong, W. Zhang, B. Liu, Synergistic dopaminergic neurotoxicity of the



- 374 pesticide rotenone and inflammogen lipopolysaccharide: Relevance to the etiology of  
375 Parkinson's disease, *The Journal of Neuroscience*. 23 (2003) 1228–1236.  
376 doi:10.1096/fj.03-0203fje.
- 377 [23] L. Deneyer, A. Massie, E. Bentea, Ketamine Does Not Exert Protective Properties on  
378 Dopaminergic Neurons in the Lactacystin Mouse Model of Parkinson's Disease,  
379 *Frontiers in Behavioral Neuroscience*. 12 (2018) 1–5. doi:10.3389/fnbeh.2018.00219.
- 380 [24] J. Blesa, I. Trigo-Damas, M. Dileone, N.L. del Rey, L.F. Hernandez, J.A. Obeso,  
381 Compensatory mechanisms in Parkinson's disease: Circuits adaptations and role in  
382 disease modification, *Experimental Neurology*. 298 (2017) 148–161.  
383 doi:10.1016/j.expneurol.2017.10.002.
- 384 [25] A.C. Vernon, S.M. Johansson, M.M. Modo, Non-invasive evaluation of nigrostriatal  
385 neuropathology in a proteasome inhibitor rodent model of Parkinson's disease, *BMC*  
386 *Neuroscience*. (2010). doi:10.1186/1471-2202-11-1.
- 387 [26] S. Mackey, Y. Jing, J. Flores, K. Dinelle, D.J. Doudet, Direct intranigral administration  
388 of an ubiquitin proteasome system inhibitor in rat: Behavior, positron emission  
389 tomography, immunohistochemistry, *Experimental Neurology*. 247 (2013) 19–24.  
390 doi:10.1016/j.expneurol.2013.03.021.
- 391 [27] J. Konieczny, A. Czarnecka, T. Lenda, K. Kamińska, E. Lorenc-Koci, Chronic l-DOPA  
392 treatment attenuates behavioral and biochemical deficits induced by unilateral  
393 lactacystin administration into the rat substantia nigra, *Behavioural Brain Research*.  
394 (2014). doi:10.1016/j.bbr.2013.12.019.
- 395 [28] H. Wang, X. Liang, X. Wang, D. Luo, J. Jia, X. Wang, Electro-Acupuncture Stimulation  
396 Improves Spontaneous Locomotor Hyperactivity in MPTP Intoxicated Mice, *PLoS*  
397 *ONE*. (2013). doi:10.1371/journal.pone.0064403.

398 **FIGURE LEGENDS**

399 **Figure 1: Four daily LPS injections induce sickness behavior.** (A-D) Sickness behavior was  
400 measured by determining changes in body weight and temperature 24 hours after each LPS or  
401 vehicle injection (Inj I-IV). (A) At the end of the four-day treatment period, LPS-treated mice  
402 had a significant decrease in body weight compared to baseline (i.e. before the first injection,  
403 time 0), contrary to vehicle-injected mice. (B) The first and second injection of LPS led to a  
404 significant decrease in body weight 24 hours after each injection, while the third and fourth  
405 injection induced an increase in body weight compared to vehicle-treatment. (C, D) Repeated  
406 LPS treatment did not induce persistent changes in body temperature as no significant  
407 differences could be observed between LPS- and vehicle-treated mice at the end or during the  
408 four-day treatment. Statistical analysis was performed using the (A, C) Wilcoxon matched  
409 paired test on the absolute values of the 96h timepoint; #### $p < 0.0001$  vs baseline, (B, D) Mann  
410 Whitney test; \* $p < 0.05$ , \*\* $p < 0.01$ , \*\*\*\* $p < 0.0001$  vs. vehicle. Arrows (Inj I-IV): i.p. injection with  
411 LPS or vehicle. **Sample size is indicated in the figure.** LPS: lipopolysaccharide, VEH: vehicle.

412 **Figure 2: Four daily LPS injections promote microglial activation.** (A) Representative  
413 images of Iba1+ stainings in the SN of vehicle and LPS-treated mice. (B) Immunohistochemical  
414 analysis of microglia in the SN revealed an increase in the number of Iba1+ cells one day after  
415 the last LPS challenge. (C) At the same timepoint, the striatal mRNA expression profile of the  
416 pro-inflammatory cytokines IL-1 $\beta$ , TNF- $\alpha$ , NOS2 and anti-inflammatory cytokine Arg1 was  
417 evaluated by real-time PCR. Repeated doses of LPS induced significant increases in IL-1 $\beta$  and  
418 Arg1. (D) Our LPS treatment paradigm did not affect striatal TH protein expression levels or  
419 (E) the number of TH+ profiles in the SNpc. Data are presented as mean  $\pm$ SEM. Statistical  
420 analysis were performed using Mann-Whitney test (B-E); \* $p < 0.05$ , \*\*\* $p < 0.01$  vs. vehicle.  
421 **Sample size is indicated in the figure.** LPS: lipopolysaccharide, Iba1: ionized calcium binding  
422 adapter molecule 1, IL-1 $\beta$ : interleukin-1 beta, TNF- $\alpha$ : tumor necrosis factor alpha, NOS2: nitric  
423 oxide synthase 2, Arg1: arginase-1. TH: tyrosine hydroxylase, VEH: vehicle. Scalebar=50 $\mu$ m.

424 **Figure 3: LPS-induced neuroinflammation enhances proteasome inhibition-induced**  
425 **degeneration of the nigrostriatal pathway.** (A) Intranigral LAC injection increases the  
426 amount of Iba1+ cells in the SN seven days after lesioning, independent of pretreatment with  
427 LPS. (B) Unilateral nigral administration of LAC significantly decreased the mean number of  
428 TH+ cells in the ipsilateral SNpc compared to sham treatment. LPS treatment prior to LAC  
429 administration resulted in a more pronounced TH+ cell loss compared to vehicle treatment. (C)  
430 Representative microphotographs of TH-staining in the SNpc in the four experimental groups.  
431 (D) LPS pre-treatment significantly increased striatal dopamine depletion and (E) dopamine  
432 turnover induced by LAC, seven days after lesioning. Data are presented as mean  $\pm$ SEM. Two-  
433 way ANOVA followed by a Tukey's *post hoc* test; \* $p < 0.05$ , \*\*\*\* $p < 0.0001$  (LAC vs sham);  
434 # $p < 0.05$  (LPS vs vehicle), § $p < 0.05$  (vs all treatment groups). **Sample size is indicated in the**  
435 **figure.** LAC: lactacystin, LPS: lipopolysaccharide, TH: tyrosine hydroxylase, Iba1: ionized  
436 calcium binding adapter molecule 1, DA: dopamine, DOPAC: 3,4-dihydroxyphenylacetic acid,  
437 HVA: homovanillic acid, VEH: vehicle. Scalebar=250 $\mu$ m.

438 **Figure 4: LAC-treated mice develop motor and non-motor symptoms.** (A) The accelerating  
439 rotarod test showed decreased time spent on the rod after LAC treatment suggesting an impaired  
440 motor coordination and balance, which was less pronounced after LPS treatment. (B)  
441 Spontaneous horizontal activity was globally increased in the open field test after LAC lesion;  
442 an effect that was enhanced by LPS pre-treatment. (C, D) Anxiety- like behavior was unaffected  
443 by LPS or LAC treatment as shown in the light-dark test and (E) the open field test. (F) LAC-  
444 induced a decrease in immobility time in the tail suspension test. Two-way ANOVA followed  
445 by a Tukey's *post hoc* test; \* $p < 0.05$ , \*\* $p < 0.01$  (LAC vs sham). Data are presented as mean  
446  $\pm$ SEM. **Sample size is indicated in the figure.** LAC: lactacystin, LPS: lipopolysaccharide, VEH:  
447 vehicle.

448 **SUPPLEMENTARY MATERIAL**

449 **Rotarod test**

450 Prior to surgery, mice were trained on a rotarod (TSE RotaRod Advanced, TSE Systems) and  
451 baseline performance was evaluated. Mice were allowed to acclimate to the testing room for 1h  
452 prior to testing. During the initial training phase, each mouse was placed on the rod at a constant  
453 speed of five rpm. When mice dropped off the rod, they were immediately placed back on the  
454 rotarod system for five consecutive min. In the second training phase, mice underwent three  
455 consecutive trials of one min at a constant speed of five rpm, with three min of rest between  
456 each trial. For evaluating rotarod performance at baseline and seven days after surgery, mice  
457 underwent five consecutive trials, each starting at five rpm for 30 seconds, followed by a five  
458 to 25 rpm accelerating protocol for 200 seconds, eventually resulting in a maximum total rod  
459 time of 230 seconds. During the test, mice were allowed to pause three min in between each  
460 trial. The mean time spent on the rod of the five trials was used for statistical analysis.

461 **Open field test**

462 Spontaneous locomotion and anxiety-like behavior were evaluated using the open field test.  
463 Mice were placed in a corner of a square box (60 cm × 60 cm; height 60 cm) with black opaque  
464 Plexiglas walls and automatically recorded for 10 min by a video tracking system (Ethovision  
465 software, Noldus). Endpoints for analysis are the spontaneous horizontal activity which is  
466 expressed as distance travelled (as a measure for spontaneous locomotion) and time spent in  
467 the center of the arena defined as the central 40 x 40 cm zone (as a measure for anxiety-like  
468 behavior).

469 **Tail suspension test**

470 The tail suspension test was used to examine depressive-like behavior. At the level of the tail  
471 suspension set-up we created an aversive illumination of 400 lux. Mice were suspended by the  
472 tip of their tail for five min to induce an inescapable situation. The time of immobility was

473 scored off-line by a blinded researcher and used as a parameter to assess depressive-like  
474 behavior. Mice that climbed their tail during the trial were excluded from the experiment.

#### 475 **Light-dark test**

476 The light-dark test investigates anxious behavior by comparing the spontaneous exploratory  
477 activity of mice with their innate aversion to well-illuminated areas. At the beginning of the  
478 experiment, each mouse was placed in a dark shelter (30 x 30 x 8.5 cm;  $\pm 0$  lux), positioned in  
479 the corner of a brightly-illuminated open field area (60 x 60 x 60 cm; 700 lux), in order to  
480 induce a conflict situation. During this experiment, two anxiety-related parameters (time spent  
481 outside the shelter and latency to exit the shelter) were manually evaluated for five min by a  
482 blinded researcher.

#### 483 **Neurochemical analysis of striatal dopamine content**

484 Striata were dissected out on an ice-cold petri dish, weighed and homogenized in 400  $\mu$ l  
485 antioxidant solution [0.05M HCl, 0.5% Na<sub>2</sub>S<sub>2</sub>O<sub>5</sub>, and 0.05% Na<sub>2</sub>EDTA], containing 10  
486 ng/100 $\mu$ l 3,4-dihydroxybenzylamine as internal standard. After centrifugation (12.000 rpm, 20  
487 min, 4 °C), the supernatant was diluted (1:5 in 0.5 M acetic acid) and stored at -80°C until use.  
488 Twenty  $\mu$ l of the diluted sample was analyzed for dopamine and the selected metabolites 3,4-  
489 dihydroxyphenylacetic acid (DOPAC) and homovanillic acid (HVA), using a narrow-bore (C18  
490 column, 5  $\mu$ m, 150 mm x 2.1 mm; Altima Grace) HPLC system with an electrochemical  
491 detector (Antec).

#### 492 **Western Blot analysis**

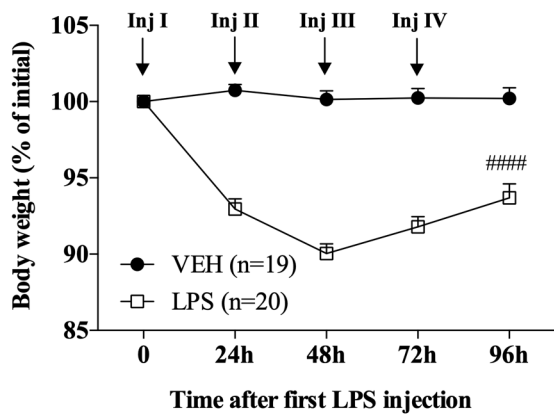
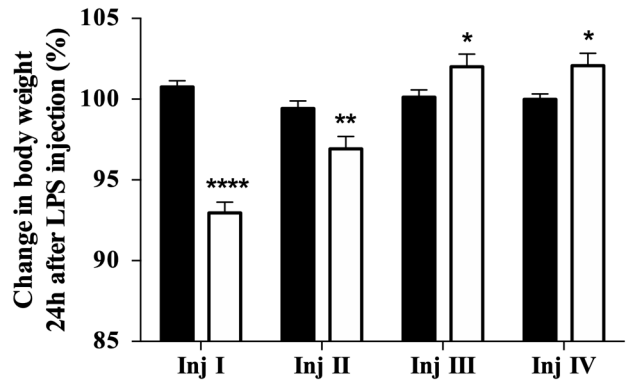
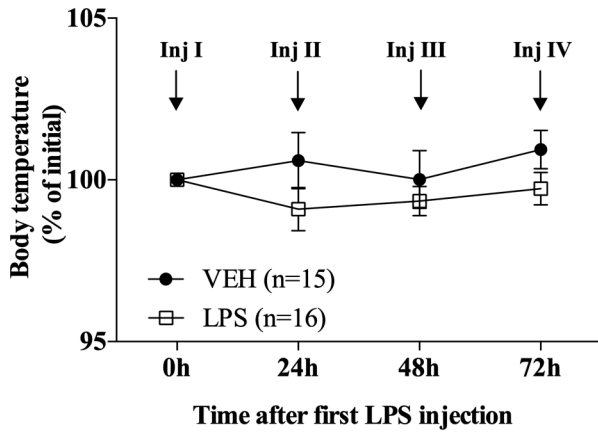
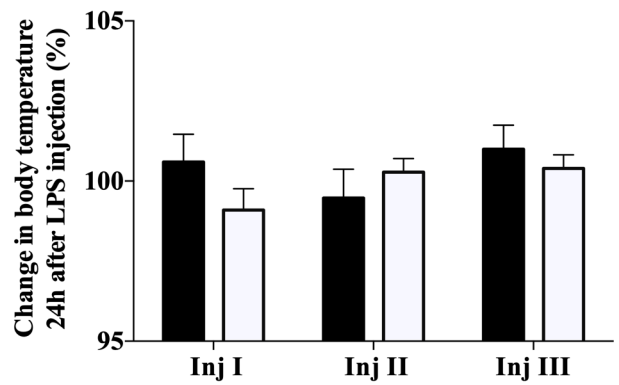
493 Striatal tissue was collected and homogenized in 300  $\mu$ l of extraction buffer (2% sodium  
494 dodecyl sulphate (SDS), 60 mM Tris base, 100 mM dithiothreitol and phosphatase & protease  
495 inhibitor cocktail (pH 6.8, Sigma-Aldrich)) and samples were incubated for 30 min at 37 °C.  
496 After centrifugation (10.000 rpm, 10 min, 4 °C), the supernatant was stored at -20 °C until use.  
497 Total protein concentration was determined using a fluorometric method (Qubit, Invitrogen,

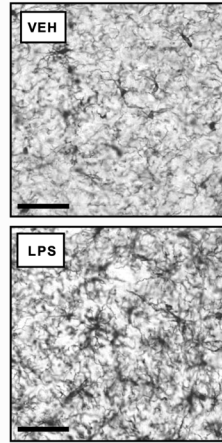
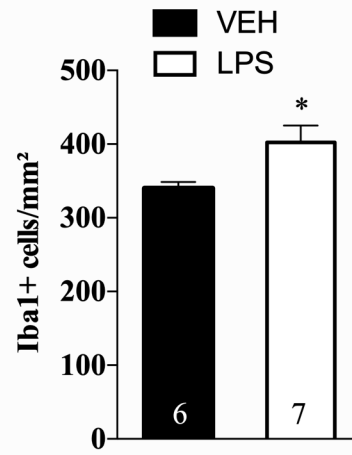
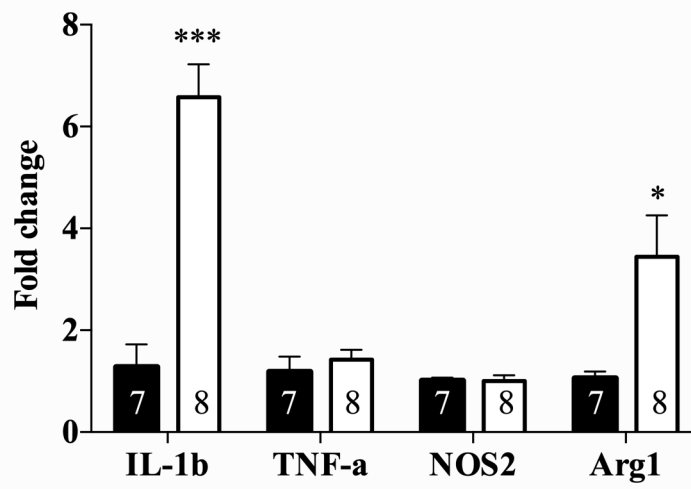
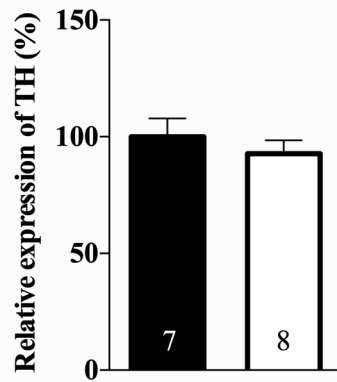
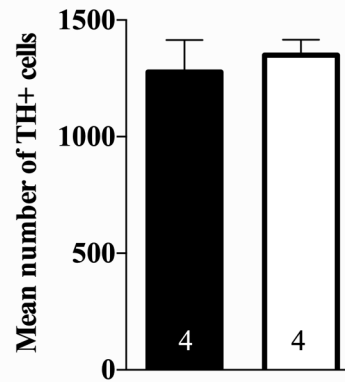
498 Life Technologies). Equal concentrations of protein were loaded on an SDS-polyacrylamide  
499 gel (4-12% gel, Bio-Rad Laboratories) in order to separate the proteins on molecular weight.  
500 Subsequently, immunoblotting was performed by transferring the proteins to a polyvinylidene  
501 fluoride membrane by means of a semi-dry system (Trans-Blot Turbo Transfer system; Bio-  
502 Rad Laboratories). Non-specific binding of the antibody was prevented by incubating the  
503 membrane in blocking agent (5% ECL Prime Membrane Blocking Agent; GE Healthcare) for  
504 at least one hour at room temperature. Afterwards, the membrane was overnight incubated at  
505 room temperature with the primary rabbit antibody. The next day, membranes were incubated  
506 with horseradish-peroxidase-conjugated anti-rabbit immunoglobulin G antiserum (1/4000,  
507 Dako) for 30 min and protein bands were visualized by enhanced chemiluminescence (ECL  
508 prime; GE Healthcare) using the LAS4000 detector (GE Healthcare). Densitometric analysis of  
509 immunopositive protein bands was done using ImageJ software (National Institute of Health)  
510 and normalized to the density of total amount of proteins loaded, visualized on the same  
511 membrane (SERVA Purple, SERVA Electrophoresis GmbH, Heidelberg, Germany).

## 512 **Real-time PCR**

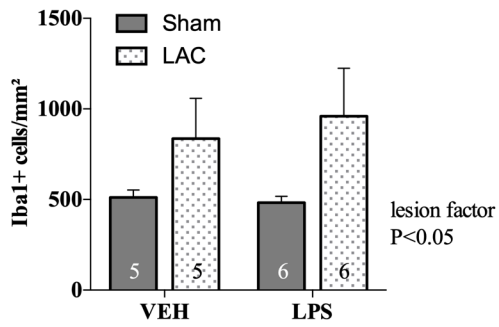
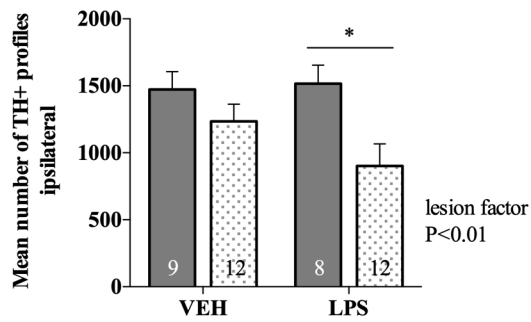
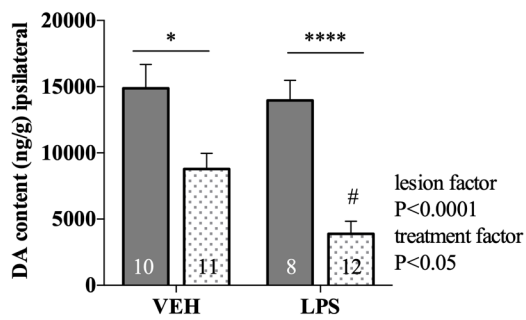
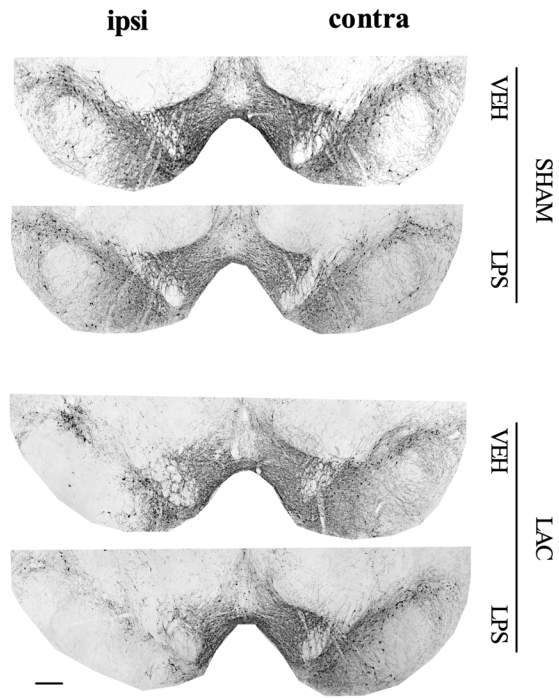
513 The qPCR reaction mix consisted of 10  $\mu$ l TaqMan<sup>®</sup> Universal Master Mix, 1  $\mu$ l of TaqMan<sup>®</sup>  
514 Gene Expression Assay and 2  $\mu$ l of cDNA in a 20  $\mu$ l volume adjusted with DNase-/RNase-free  
515 water. The TaqMan<sup>®</sup> Gene Expression Assays used were the following: IL-1 $\beta$  (assay ID:  
516 Mm00434228\_m1), TNF- $\alpha$  (assay ID: Mm00443258\_m1), Nos2 (assay ID:  
517 Mm00440502\_m1), Arg1 (assay ID: Mm00475988\_m1), Ywhaz (assay ID: Mm03950126\_s1),  
518 Brap (assay ID: Mm00518493\_m1) and Bcl2l13 (assay ID: Mm00463355\_m1). Bcl2l13 was  
519 identified as the most stable housekeeping gene of the three housekeeping genes tested (Ywhaz,  
520 Brap and Bcl2l13) using Normfinder.

521

**A****B****C****D**

**A****B****C****D****E**



**A****B****D****C****E**